Persistence as an optimal hedging strategy

Alexander P Browning[1,2,*], Jesse A Sharp[1,2], Tarunendu Mapder[1,2,3], Christopher M Baker[1,2,4], Kevin Burrage[1,2,5], and Matthew J Simpson[1]

[1] *School of Mathematical Sciences, Queensland University of Technology, Australia*
[2] *ARC Centre of Excellence for Mathematical and Statistical Frontiers, QUT, Australia*
[3] *Department of Medicine, Indiana University School of Medicine, Indianapolis, U.S.A.*
[4] *School of Mathematics and Statistics, University of Melbourne, Australia*
[5] *Department of Computer Science, University of Oxford, UK*

July 3, 2020

Abstract

Bacteria invest in a slow-growing subpopulation, called *persisters*, to ensure survival in the face of uncertainty. This hedging strategy, which we term *cellular hedging*, is remarkably similar to financial hedging where diversifying an investment portfolio protects against economic uncertainty. We provide a new theoretical foundation for understanding cellular hedging by unifying the study of biological population dynamics and the mathematics of financial risk management. Our approach explicitly incorporates environmental volatility as a stochastic process, and we study the persister strategy that maximises the expected per-capita growth rate by formulating a stochastic optimal control problem. We demonstrate that persistence is only advantageous in the presence of environmental volatility. Analytical and simulation results probe the optimal persister strategy, revealing results that are consistent with experimental observations and suggest new opportunities for experimental investigation. Overall, we provide a new way of conceptualising and modelling cellular decision making by unifying previously disparate theory from mathematical biology and finance.

Keywords: persisters, bet-hedging, optimal control, financial mathematics, antibiotic resistance, stochastic growth

Introduction

Shortly after the clinical introduction of penicillin, Bigger noticed a resistance in a small subpopulation of *Staphylococcal pyogenes* (1). The resistant cells, termed *persisters*, are a genetically identical, slow-growing, phenotypic variant. Bacteria invest in persisters to ensure survival: persisters are less proliferative than regular cells in a nutrient rich environment but can withstand adversity (2). These strategies are akin to financial hedging, where diversifying an investment portfolio protects against economic uncertainty (3–6). This type of strategy in biology and ecology is commonly referred to as *bet-hedging* (2, 5, 7–9).

Bacterial persistence poses a significant clinical challenge and is highly advantageous to bacteria. For example, persisters are less sensitive to antibiotic treatment (10–13), are undetectable in routine clinical tests (14), and are thought to be responsible for the formation (15) and incurability (16) of many infections. Antimicrobial treatments will, therefore, benefit from an understanding of how persisters arise and function (17). The similarity between bacterial persistence and financial hedging strategies suggests a new pathway to investigate persister dynamics. In this study, we provide a novel, quantitive understanding of persister strategies using techniques from financial mathematics and stochastic optimal control theory. Persister production is known to depend on the environment (10, 18, 19) and our mathematical modelling approach allows us to unearth how various optimal persister strategies depend upon environmental volatility.

Persisters can be revealed experimentally by disinfecting a population of *Escherichia coli* (*E. coli*) with ampicillin, which targets proliferative cells (10). The initially rapid reduction in population size eventually slows, revealing a small subpopulation that is less sensitive to the treatment. Experimental investigations are complicated by the extreme scarcity of persister cells: typically less than 1 in 10^5 cells are persisters in wild type *E. coli* (20). For subpopulations of this size, stochastic effects are significant (21, 22).

In producing persisters, bacteria allocate resources to hedge against environmental volatility for the purpose of survival. Our hypothesis is that these processes occur in much the same way that a financial investor hedges a portfolio to protect from, and take advantage of, economic volatility. We refer to our approach as *cellular hedging* due to the explicit link between our modelling framework and both financial hedging and optimal control. The archetypal example of portfolio diversification is Merton's portfolio problem (MPP) (3). Here, an investor allocates a fraction of their wealth in a high-yield volatile asset, such as stocks; and a low-yield stable asset, such as government bonds. Stochastic optimal control theory (23) is used to maximise the investors wealth by modelling the proportion allocated to each asset as a *control*. Merton's work reveals that it is not advantageous to possess the low-yield asset in the absence of uncertainty, or when the growth of the high-yield asset is deterministic. MPP revolutionised the field of mathematical finance, and many of the ideas in MPP formed the basis of Merton's later work on options pricing (24, 25) that led to the the 1997 Nobel Prize in Economics.

An existing class of mathematical models focusing on hedging in cell biology describe environmental uncertainty by transiting the growth rate through finitely many states (such as growth and stress), where transitions occur either periodically (8, 21, 26) or stochastically (4, 5, 27). These studies maximise some measure of the long-term growth rate of the population and probe the environmental conditions under which persistence is advantageous. A drawback to these existing modelling approaches is their inability to capture other models of stochastic environmental volatility. In our study, we model persistence under the arguably simpler assumption of a growth rate subject to continuous stochastic fluc-

*Corresponding author. E-mail: ap.browning@qut.edu.au

tuations, which we model using Wiener noise (22, 23). Our approach is also able to incorporate more complex stochastic models of the environment. The models of environmental volatility we study in this manuscript include, for example, Poisson jump noise (28), which is able to capture the aforementioned existing models of environmental volatility (4, 5, 8, 21, 27) where transitions in the growth rate occur due to, for example, shocks.

In this work, we develop a new framework for studying cellular hedging at the population level by unifying two previously disparate fields: biological population dynamics and financial mathematics. The reason we use the term *cellular hedging*, instead of the term *bet-hedging* (2, 5, 7–9), is the direct connection with optimal control from financial modelling. We describe bacteria growth using a stochastic model that explicitly incorporates environmental volatility as a stochastic process. This is the first time that bacterial persistence has been described at the population level using a stochastic differential equation model. Furthermore, in order to probe the persister strategy that maximises the per-capita growth of the bacteria colony, we apply stochastic optimal control theory (23, 28). A fundamental result of our study indicates that investing in persisters is only advantageous in the presence of environmental volatility (6) , suggesting study of bacterial persistence warrants a stochastic model. Our new model and approach leads to mathematical results that are consistent with observations from several key experimental studies, and provides new insights into bacteria dynamics in the face of environmental volatility.

Methods

Stochastic model of bacteria growth

We model population-level bacteria dynamics with a system of Itô stochastic differential equations (SDEs) driven by Wiener noise (6, 22, 23). This choice of model can be thought of as a bridge between discrete Markov models (21), and continuous ordinary differential equation (ODE) models (10). In addition, our population-level model of bacterial persistence complements stochastic gene expression models that describe the regulation of persister strategies (6, 29). Further, we model the dynamics of bacteria in a volatile environment by coupling the growth rate to a stochastic process representing the environment (30).

We model the population of regular (non-persister) cells, r_t, and persisters, p_t. Here, a subscript t indicates that each stochastic processes depends on time, t. The growth of regular cells is described by an Itô SDE such that the net growth rate, μ_t, is subject to stochastic fluctuations characterized by a Wiener process scaled by an intensity σ (22). The quiescence of persisters manifests slow metabolic activity, so we assume the growth rate of persisters is some small proportion, $\varepsilon < 1$, that of regular cells. The net persister growth rate is subject to stochastic fluctuations characterized by a Wiener process scaled by an intensity $\eta = \varepsilon\sigma$. Many other choices for a stochastic population dynamics model exist (22), such as where the fluctuations vanish for large population sizes (21). However, the focus of our work is on fluctuations in the environment and growth rate, which we assume to be independent of the population size.

The current literature classifies two types persister production in a population: variable and environment dependent, commonly referred to as Type I; or constant, commonly referred to as Type II (10) (Fig. 1). It is understood that constant production of persisters, which results in an approximately constant proportion in a growing population, may be

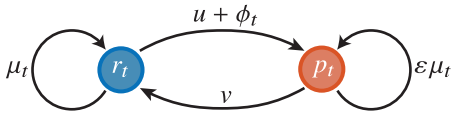

Fig. 1. Schematic of the bacteria growth model with regular cells, r_t, and persisters, p_t. Switching from persisters to regular cells is constant, v. Switching from regular cells to persisters is taken to be the sum of a constant rate, u, and a variable rate, ϕ_t, that depends upon environmental volatility.

regulated by stochastic gene fluctuation on a single cell level (31–33). In addition, a growth feedback mechanism (34) — possibly regulated by quorum sensing (35) and intercellular signalling (36) — may enable cells to respond and vary the persister production rate. In our model, regular cells switch to persisters at a rate of $u+\phi_t$, where: $u \geq 0$ is the constant rate (10); and $\phi_t \geq 0$ is the variable, environment-dependent, rate. Persisters revert to regular cells at a constant rate $v \geq 0$. Our model can, therefore, describe both Type I and Type II strategies.

These dynamics give rise to a system of Itô SDEs

$$\mathrm{d}r_t = \mu_t r_t \,\mathrm{d}t + \sigma r_t \,\mathrm{d}W_t^{(1)} - \big[(u+\phi_t)r_t - vp_t\big]\,\mathrm{d}t\,, \tag{1a}$$

$$\mathrm{d}p_t = \underbrace{\varepsilon\mu_t p_t \,\mathrm{d}t + \eta p_t \,\mathrm{d}W_t^{(2)}}_{\text{Subpopulation growth}} + \underbrace{\big[(u+\phi_t)r_t - vp_t\big]\,\mathrm{d}t}_{\text{Phenotype switching}}\,. \tag{1b}$$

Here, $W_t^{(1)}$ and $W_t^{(2)}$ are two independent Wiener processes that satisfy $W_{t+h}^{(i)} - W_t^{(i)} \sim \mathcal{N}(0,h)$, $h > 0$, $i = 1,2$ where $\mathcal{N}(0,h)$ denotes a normal distribution with mean zero and variance h. Such a system of equations is said to be in the form of multiplicative Wiener noise (28). We note that in removing variability from the model by setting $\sigma = \eta = 0$, we recover the ODE model of Balaban *et al.* (10).

We find it natural to consider the variable transformation

$$n_t = r_t + p_t, \quad \theta_t = p_t \,/\, n_t, \tag{2}$$

such that n_t represents the population size and θ_t represents the proportion of persisters. Following Itô's lemma (23), the transformed state equations are

$$\begin{aligned}\mathrm{d}n_t &= \big[1-\theta_t(1-\varepsilon)\big]\mu_t n_t\,\mathrm{d}t \\ &\quad + \sigma n_t(1-\theta_t)\,\mathrm{d}W_t^{(1)} + \eta n_t\theta_t\,\mathrm{d}W_t^{(2)}\,,\end{aligned} \tag{3a}$$

$$\begin{aligned}\mathrm{d}\theta_t &= \big[(1-\theta_t)(u+\phi_t) - \theta_t v - (1-\theta_t)\theta_t\big((1-\varepsilon)\mu_t \\ &\quad - \sigma^2(1-\theta_t) + \eta^2\theta_t\big)\big]\,\mathrm{d}t \\ &\quad - (1-\theta_t)\theta_t\sigma\,\mathrm{d}W_t^{(1)} + \eta(1-\theta_t)\theta_t\,\mathrm{d}W_t^{(2)}\,,\end{aligned} \tag{3b}$$

revealing that the dynamics of the persister proportion, θ_t, are independent of the population size, n_t.

Stochastic model environmental volatility

We model environmental volatility by assuming $\mu_t = m(\zeta_t)$, where ζ_t is a stochastic process that represents a volatile environment. There are many appropriate choices for $m(\cdot)$ and ζ_t, but we focus our analysis on three environments, samples paths of each shown in Fig. 2*a*–*c*. These are

1. *Constant.* (Fig. 2*a*) We set $m(\zeta) \in \{\mu_G, \mu_S\}$, such that μ_t is constant. Here μ_G represents a colony during growth; and μ_S represents a colony under stress or specifically, antimicrobial treatment. For numerical results, we choose $\mu_G = 2\,\mathrm{h}^{-1}$ and $\mu_S = -2\,\mathrm{h}^{-1}$ to match experimental data for *E. coli* during growth and ampicillin treatment (10).

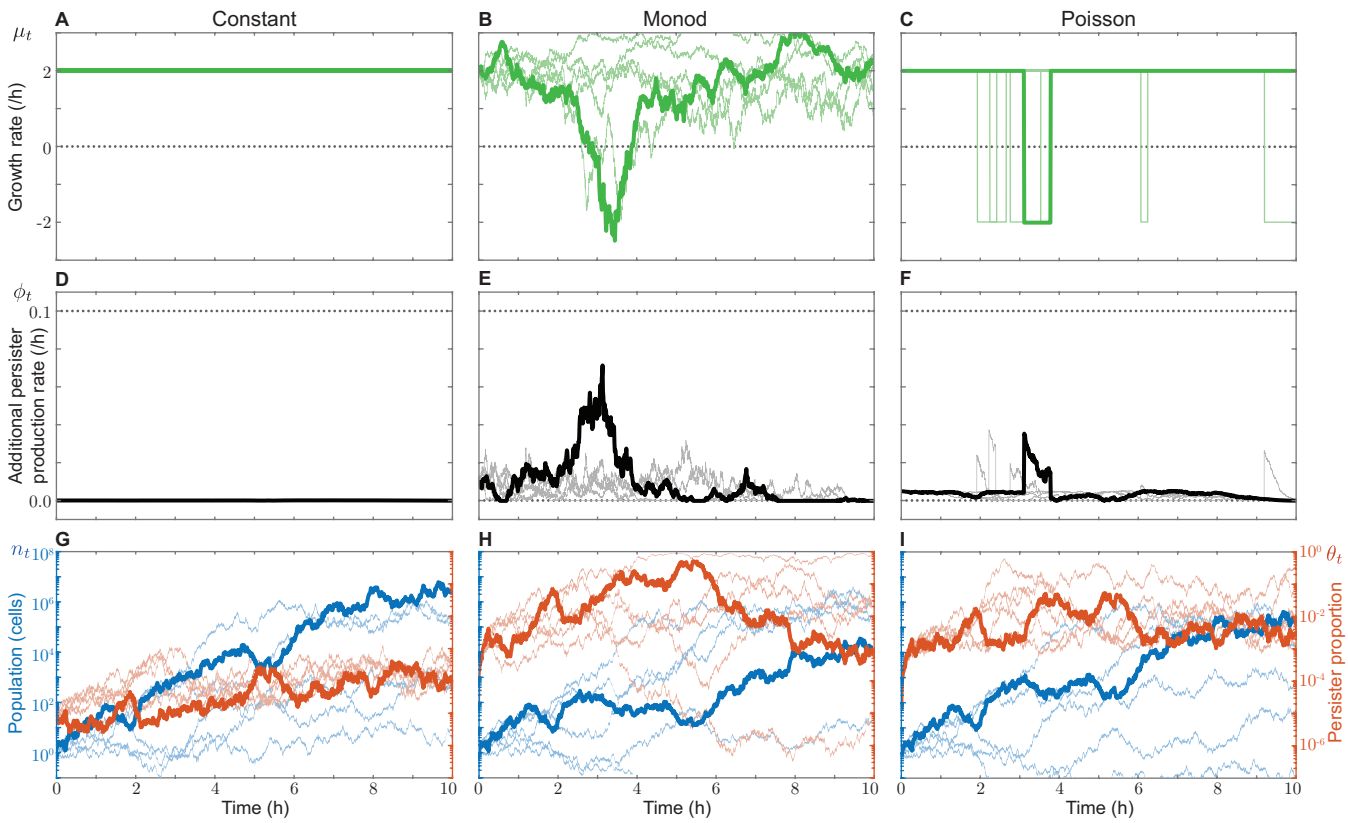

Fig. 2. Optimal persister production in cell populations under various types of environment. (a)-(c) Growth rates, μ_t, sampled from each environment to simulate bacteria growth in the rest of the figure. (d)-(f) The variable persister production rate, ϕ_t^*, for a single realisation of the model. (g)-(i) The population, n_t, (blue, left scale) and persister proportion, θ_t, (red, right scale), for a single realisation of the model. The seeds used to generate the Wiener processes $W_t^{(1)}$ and $W_t^{(2)}$ are identical for all environments. Also shown are five additional, independent, realisations (semi-transparent).

2. *Monod.* (Fig. 2*b*) Monod kinetics are commonly used to model the growth of bacteria (37–39), and feature dynamics with an asymptotic upper bound on the growth rate, but no lower bound. We describe this environment by a mean-reverting Ornstein-Uhlenbeck process (23) and couple the growth rate using a Monod equation (37),

$$m(\zeta_t) = \frac{\mu_{\max}\zeta_t}{K_\zeta + \zeta_t} - \delta, \tag{4a}$$

$$\mathrm{d}\zeta_t = \xi(K_\zeta - \zeta_t)\,\mathrm{d}t + \kappa\,\mathrm{d}W_t^{(3)}\,, \tag{4b}$$

where $W_t^{(3)}$ is a Wiener process independent of both $W_t^{(1)}$ and $W_t^{(2)}$. Here, ζ_t experiences fluctuations proportional to κ and a reversion force to the state $\zeta_t = K_\zeta$ of strength proportional to ξ. The Monod coupling features an asymptotic upper-bound on the growth rate of $\mu_t = \mu_{\max}$ and no lower bound. Unfavourable environmental changes have, therefore, a larger effect on the growth rate than those that are favorable, and the growth rate experiences reversion to a growth rate $\mu_t = \mu_{\max}/2 - \delta$, where δ represents the natural death rate. For numerical results, we choose $\xi = 0.1\,\mathrm{h}^{-1}$, $K_\zeta = 1$, $\zeta_0 = 1$, $\kappa = 0.3$, $\mu_{\max} = 8\,\mathrm{h}^{-1}$ and $\delta = 2\,\mathrm{h}^{-1}$. For this choice of parameters the growth rate experiences reversion to a growth rate of $\mu_G = 2\,\mathrm{h}^{-1}$, which corresponds to the constant environment. To deal with the discontinuity at $\zeta = -K_\zeta$, we truncate Eq. 4a so that $m(\zeta) = m(-0.5)$ for $\zeta < -0.5$.

3. *Poisson.* (Fig. 2*c*) An existing class of mathematical models describe environmental uncertainty using alternating periods of growth and stress (4, 5, 8, 21, 27). We reproduce this type of environment in a stochastic model by assuming that the environment switches between growth and stress according to a Poisson process. We consider that $m(\zeta) = \mu_G$ for $\zeta \geq 0$; $m(\zeta) = \mu_S$ for $\zeta < 0$; and model the environment as the Poisson jump process (28)

$$\mathrm{d}\zeta_t = \rho(\zeta_t)\,\mathrm{d}P_t\,, \quad \mathrm{d}P_t \sim \mathrm{Po}(\mathrm{d}t\,\lambda(\zeta_t)), \tag{5a}$$

$$\text{where } \rho(\zeta_t) = \begin{cases} -2, & \zeta_t = +1, \\ +2, & \zeta_t = -1, \end{cases} \tag{5b}$$

$$\text{and } \lambda(\zeta_t) = \begin{cases} 1/\tau_G, & \zeta_t = +1, \\ 1/\tau_S, & \zeta_t = -1. \end{cases} \tag{5c}$$

This formulation allows for a mean time of τ_G in the growth phase, where $\mu_t = \mu_G$, and a mean time of τ_S in the stress phase, where $\mu_t = \mu_S$. For numerical results in this study, we choose $\tau_G = 9.5\,\mathrm{h}$, $\tau_S = 0.5\,\mathrm{h}$, $\zeta_0 = 1$, $\mu_G = 2\,\mathrm{h}^{-1}$ and $\mu_S = -2\,\mathrm{h}^{-1}$.

These choices represent environments in which changes happen gradually (Monod environment) or abruptly (Poisson environment), as demonstrated in Fig. 2*b* and Fig. 2*c*, respectively. For comparative purposes we choose similar realisations of each environment and choose the initial condition for all environments such that $\mu_0 = \mu_G = 2\,\mathrm{h}^{-1}$. In the supporting material, we explore results for two other models of environmental volatility: (4) an Ornstein-Uhlenbeck process without a Monod coupling (Fig. S1d) and, (5) a Duffing oscillator (Fig. S1e).

Optimal persister production strategies

Our ideas of *cellular hedging* suggest that a cell population chooses a persister production strategy $\mathcal{S} = \{u, v, \phi_t\}$ that is optimal in some way. Mathematically, we define optimality as the strategy that maximises some *fitness measure*, which we now construct. We assume that there is no explicit cost to producing persisters with constant rates u and v; but that there is a quadratic running cost to produce persisters with a variable rate ϕ_t. The cost of applying a non-zero ϕ_t accounts for the sensing mechanisms that cells must use to respond to the environment.

We choose a fitness measure, commonly referred to as a *payoff* in optimal control theory, as

$$J_{\mathcal{S}} = \mathbb{E}\Bigg[\underbrace{\int_0^T \alpha\phi_t^2 \,\mathrm{d}t}_{\text{Sensing}} + \underbrace{\log_{\mathrm{e}}(n_T)}_{\text{Growth}}\Bigg],\ \alpha < 0. \tag{6}$$

Here T denotes a terminal time, so that the maximisation is carried out on the interval $t \in [0, T]$; and, $\alpha < 0$ characterises a trade-off between growth and operating the sensing mechanisms required to vary the persister production rate. The terminal time might correspond to, for example, the duration of the growth phase for the population (10). Maximising the logarithmic term in Eq. 6 can be interpreted as cells maximising their per-capita growth rate over the interval $t \in [0, T]$, since

$$\log_{\mathrm{e}}(n_T) = \log_{\mathrm{e}}(n_0) + \int_0^T \frac{1}{n_t}\frac{\mathrm{d}n_t}{\mathrm{d}t}\,\mathrm{d}t\,,$$

and $\log_{\mathrm{e}}(n_0)$ is constant (40). Our choice of fitness measure corresponds to evolutionary mechanisms that perpetuate highly productive populations (21). There are many other choices of fitness, such as resource allocation based on a maximum entropy principle (41). We expect our methodology to carry across to these more complicated choices of fitness measure.

Together with the state equations (Eq. 3), maximising Eq. 6 corresponds to an optimal control problem. We apply Hamilton-Jacobi-Bellman (HJB) optimal control theory (23, 28) to reformulate the optimal control problem as a partial differential equation (PDE) problem. We now review essential elements of Hamilton-Jacobi-Bellman (HJB) optimal control theory.

Review of optimal control theory

A stochastic control problem may be stated as

$$\max_{\omega_t \in \mathcal{U}} \mathbb{E}\left(\int_0^T \mathcal{L}(\mathbf{x}_t, \omega_t, t)\,\mathrm{d}t + \Phi(\mathbf{x}_T)\right), \tag{7}$$

where ω_t is the control from the set of allowable controls, $\mathcal{U}$. The state equations are given by the q-dimensional stochastic process, $\mathbf{x}_t$, governed by

$$\mathrm{d}\mathbf{x}_t = \mathbf{M}(\mathbf{x}_t, \omega_t, t)\,\mathrm{d}t + \mathbf{\Sigma}(\mathbf{x}_t, \omega_t, t)\,\mathrm{d}\mathbf{W}_t\,, \tag{8}$$

where $\mathbf{M} \in \mathbb{R}^q$ gives the drift of the process; $\mathrm{d}\mathbf{W}_t \in \mathbb{R}^q$ is a Wiener process of the same dimension as $\mathbf{x}_t$ with independent constituants; and, $\mathbf{\Sigma}\mathbf{\Sigma}^{\mathrm{tr}} \in \mathbb{R}^{q\times q}$ describes the covariance of the Wiener process (superscript ^{tr} denotes the matrix transpose). In this study, we also study a form of $\mathbf{x}_t$ that includes Poisson jump noise, and we include the derivation of the HJB equations for this case in the supporting material.

To solve the optimal control problem we define the value function, $V(\mathbf{x}, s)$, as the optimal payoff obtainable starting at $\mathbf{x}$ at time s and continuing to terminal time T. That is,

$$V(\mathbf{x}, s) = \max_{\omega_t \in \mathcal{U}} \mathbb{E}\left(\int_s^T \mathcal{L}(\mathbf{x}_t, \omega_t, t)\,\mathrm{d}t + \Phi(\mathbf{x}_T)\right), \quad \text{subject to } \mathbf{x}_s = \mathbf{x}. \tag{9}$$

Hamilton-Jacobi-Bellman (HJB) theory describes V as the solution of a partial differential equation (PDE) (23, 28), given by

$$0 = \max_{\omega_t \in \mathcal{U}} \left(\mathcal{A}V + \mathcal{L}(\mathbf{x}_t, \omega_t, t)\right), \tag{10}$$

where $\mathcal{A}$ is the stochastic generator for the process governing $\mathbf{x}_t$. For the q-dimensional system given by Eq. 8, the stochastic generator is given by

$$\mathcal{A}V = \frac{\partial V}{\partial s} + \sum_{i=1}^{q}\left(\mathbf{M}_i\frac{\partial V}{\partial x_i} + \frac{1}{2}\sum_{j=1}^{q}(\mathbf{\Sigma}\mathbf{\Sigma}^{\mathrm{tr}})_{ij}\frac{\partial^2 V}{\partial x_i \partial x_j}\right) \tag{11}$$

where $\mathbf{M}_i$ denotes the ith element of $\mathbf{M}(\mathbf{x}_t, \omega_t, t)$, and $(\mathbf{\Sigma}\mathbf{\Sigma}^{\mathrm{tr}})_{ij}$ denotes the element in the ith row and jth column of $\mathbf{\Sigma}\mathbf{\Sigma}^{\mathrm{tr}}$, for $\mathbf{\Sigma} = \mathbf{\Sigma}(\mathbf{x}_t, \omega_t, t)$. Substituting the terminal time $s = T$ into Eq. 9 provides the terminal condition $V(\mathbf{x}, T) = \Phi(\mathbf{x}_T)$.

In certain cases, the argmax$(\mathcal{A}V + \mathcal{L})$ term in Eq. 10 may be found analytically through differentiation. This yields both an expression for the optimal control, ω_t^*; and a q-dimensional, non-linear, PDE coupled to a terminal condition. In the case of MPP, Eq. 10 has an analytical solution (3), however in most cases we are required to solve Eq. 10 numerically. To obtain an optimal trajectory starting at state $\mathbf{x}_0$, we solve the state equations (Eq. 8), coupled to the solution of the HJB PDE (Eq. 10), forward in time using the Euler-Maruyama algorithm (42). Full details of the numerical techniques are provided in the supporting material.

Numerical methods to solve the SDEs

We integrate the SDE models using the Euler-Maruyama algorithm (42) with time step $h = 2\times10^{-3}$. To compare results between environments, we fix the seeds used to generate the Wiener processes $W_t^{(1)}$ and $W_t^{(2)}$ when simulating different models. Full details of the numerical method used to solve the SDEs are given in the supporting material.

Constant persister production

We first examine a population that can only produce persisters at a constant rate, so we fix the variable rate, $\phi_t = 0$. In this case, we only assume the constant environment so $\mu_t = \mu_G$.

As u and v only appear in the optimal control problem linearly, the solution is not finite unless a bound is enforced on u and v (43). The unbounded problem corresponds to a cell population that is able to move itself instantaneously to anywhere in the state space. To address this, we assume that the constant switching rates u and v are chosen by the population to control the steady-state persister proportion, which we denote $\hat{\theta}_t \in [0, 1]$. Taking the drift term in the state equation for θ_t (Eq. 3b) to be zero, we see that u and v are related to $\hat{\theta}_t$ by

$$u = \hat{\theta}_t\left(\frac{v}{1-\hat{\theta}_t} + \eta^2\hat{\theta}_t - (1-\hat{\theta}_t)\sigma^2 + (1-\varepsilon)\mu_G\right). \tag{12}$$

At this point, we note that Eq. 12 is only consistent if $\hat{\theta}_t$ is constant, and we address this shortly.

Allowing $\hat{\theta}_t$ to be a control, the state equation for n_t (Eq. 3a) becomes

$$\frac{\mathrm{d}n_t}{n_t} = (1-\hat{\theta}_t(1-\varepsilon))\mu_G\,\mathrm{d}t + \sqrt{(1-\hat{\theta}_t)^2\sigma^2 + \hat{\theta}_t^2\eta^2}\,\mathrm{d}W_t\,, \quad (13)$$

since $a\,\mathrm{d}W_t^{(1)} + b\,\mathrm{d}W_t^{(2)}$ can be considered as $\sqrt{a^2+b^2}\,\mathrm{d}W_t$. Assuming that $\hat{\theta}_t$ is chosen to maximise the fitness measure (Eq. 6) reveals a problem closely related to MPP (3). The problems differ intrinsically in that an investor is able to reallocate assets within a financial portfolio instantaneously and without cost — though variations of MPP address this — whereas the cell colony comprises finitely many cells that act heterogeneously using finite switching rates to produce persisters.

We apply stochastic optimal control theory (23, 28) and exploit the similarity between this formulation of the persister problem and MPP (3) to obtain an analytical solution, in which the optimal control, denoted $\hat{\theta}_t^* \in [0,1]$, is given by

$$\hat{\theta}_t^* = \max\left[0, \min\left(1, \frac{\sigma^2 - (1-\varepsilon)\mu_G}{\eta^2+\sigma^2}\right)\right]. \quad (14)$$

Full details of this analytical solution are given in the supporting material. As is the case with MPP, $\hat{\theta}_t^*$ is constant, so the strategy is independent of both the time and system state. Solving Eqs. 12 and 14 simultaneously gives $\hat{\theta}_t^* = 1.19\times10^{-5}$ with $\sigma = 1.414222$ which matches experimental observations for wild type *E. coli* bacteria where $\mu_G = 2\,\mathrm{h}^{-1}$, $\varepsilon = 0$, $\eta = \varepsilon\sigma = 0$, $u = 1.2\times10^{-6}\,\mathrm{h}^{-1}$ and $v = 0.1\,\mathrm{h}^{-1}$ (10). For numerical results in the rest of this study, we fix σ, ε, η, u and v to these values, and set the initial persister proportion $\theta_0 = 1.19\times10^{-5}$.

Variable persister production

We now consider a cell colony that is able vary persister production in response to their environment. In this case, $\phi_t \in \mathbb{R}^+$, can be thought of as a Markovian control (23), or a control that is chosen based on information that includes the current state and time, but does not carry a memory about the past state. For numerical stability, we place an upper-bound on the control such that $\phi_t \le 0.1\,\mathrm{h}^{-1}$.

To solve the control problem, we define the value function, V, by

$$V(x,y,z,s) = \max_{\phi_t} \mathbb{E}\left[\int_s^T \alpha\phi_t^2\,\mathrm{d}t + \log_\mathrm{e}(n_T)\right], \quad (15a)$$

$$\text{where} \quad (n_s,\theta_s,\zeta_s) = (x,y,z). \quad (15b)$$

HJB optimal control theory describes V with a PDE, details of which are given in Materials and Methods. In our case, we can express this PDE as

$$0 = \max_{\phi_t}\left(\alpha\phi_t^2 + \frac{\partial V}{\partial y}\phi_t + \mathcal{H}_\star\right), \quad (16)$$

where $\mathcal{H}_\star$ represents a collection of terms independent of the control, ϕ_t. As Eq. 16 is quadratic in ϕ_t, we can carry out the maximisation by setting the derivative to zero to find the optimal control, denoted $\phi_t^* \in [0, 0.1]$, as

$$\phi_t^* = \max\left[0, \min\left(0.1, -\frac{1}{2\alpha}\frac{\partial V}{\partial y}\right)\right]. \quad (17)$$

Here, $y = \theta_t$ is the current persister proportion. Since $y \in [0,1]$, an interpretation of Eq. 17 is that the population uses ϕ_t^* to steer the population toward the optimal persister proportion, where $\partial V/\partial y = 0$. As environmental triggers only create persisters (the quiescent state of persisters means they are unable to react to the environment), $\phi_t^* > 0$, and so ϕ_t^* is only active if the current proportion is less than the optimal proportion. Finally, $\phi_t^* \to 0$ as $\alpha \to -\infty$, which represents the sensing mechanisms becoming prohibitively expensive.

Substituting Eq. 17 into the HJB equation leads to a nonlinear PDE for V that must be solved backward in time. Full details of this equation are given in the supporting material. In summary, the variable transformation $x \to \log_\mathrm{e}(x)$ removes all terms containing the independent variable x (representing the current population size) from the equation. Therefore, we find that the ansatz

$$V(x,y,z,s) = \Psi(y,z,s) + \log_\mathrm{e}(x), \quad (18)$$

is consistent with the system. This result reveals that the optimal control (Eq. 17) is independent of the population size since $\partial V/\partial y = \partial\Psi/\partial y$. This gives an optimal strategy of the form $\phi_t^* = \phi^*(t,\theta_t,\zeta_t)$. These results suggest that bacteria can implement an optimal variable persister strategy using only information about the proportion of persisters (through, for example, quorum-sensing (35) or intercellular signalling (36)), and the environment (through, for example, a growth feedback mechanism (34)). Therefore, the persister strategy is dependent upon stochastic fluctuations in both the proportion of persisters and the environment.

In Fig. 2 we show dynamics for cell colonies in all three environments for $\alpha = -100\,\mathrm{h}$. For these results, we solve for Ψ numerically. As expected, we find that unfavorable environments trigger variable persister production (Fig. 2*e,f*), without any additional persister production for the constant environment (Fig. 2*d*). This suggests that a constant persister production strategy is sufficient for an environment with a constant expected growth rate. On the other hand, additional persister production is seen in response to environmental cues for more volatile environments (Fig. 2*e,f*). An interesting result in Fig. 2*e* is that the peak variable production rate under the Monod environment lies before the minimum growth rate. This suggests that the model implicitly incorporates mechanisms such that cells understand the environment to the extent that they can anticipate environmental changes, perhaps based on past events or sudden changes in the environment.

Behaviour under unfamiliar environments and antimicrobial treatment

By assuming that cells monitor their growth rate, μ_t, we can explore how bacteria that are specialised to one environment (i.e. implement the optimal persister strategy) behave under an unfamiliar environment. We couple the growth rate to the optimal control by considering $\phi_t^* = \phi^*(\theta_t,\zeta_t)$ where $\zeta_t = m^{-1}(\cdot)$ denotes the inverse of the growth rate coupling function $m(\zeta)$. In other words, the cells measure the current environment state using the growth rate.

Persisters are revealed experimentally by exposing the population to antibiotics and monitoring the population size (10). We simulate this process to examine how bacteria specialised to each environment behave when exposed to a constant expected decay rate. Simulation results in Fig. 3*a*, for a population that can only produce persisters at a constant rate, are similar to experimental results for wild-type *E. coli* (10). In comparison, we find that colonies that implement a strategy optimal under a more volatile environment, such as the Poisson and Monod environments, produce persisters using the variable rate (Fig. 3*c*) reach saturation of persisters more quickly (Fig. 3*b*) and have a higher long term population (Fig. 3*a*). These qualitative observations suggest

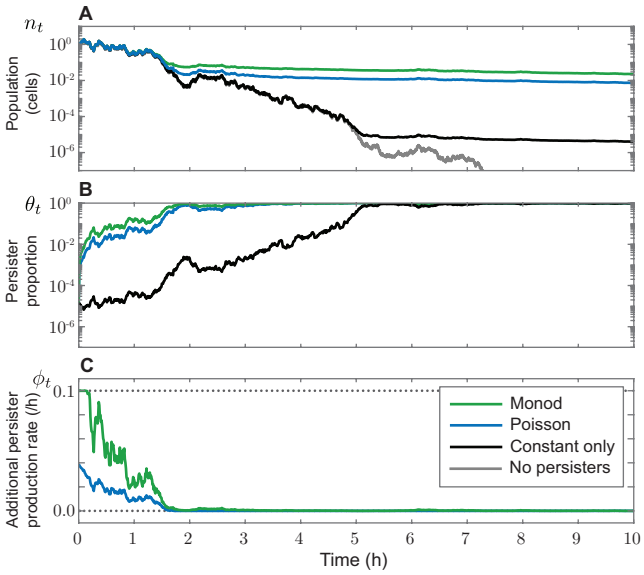

Fig. 3. Single realisations of the model showing the behaviour of a cell population under antibiotic treatment. (a) Shows the population, n_t; (b) shows the persister proportion, θ_t; and, (c) shows the variable persister production rate, ϕ_t^*. In all cases, the cells experience a growth rate $\mu_t = -2\,\mathrm{h}^{-1}$ and implement: the variable strategy optimal under either the Monod environment (green) or the Poisson environment (red); constant switching only optimal under the constant environment (black); or do not produce persisters (grey).

that high persistence bacteria strains (10, 21) could arise in response to highly volatile environments. In the supplementary material we apply the same methodology to simulate bacteria specialised to each environment under other, unfamiliar, environments. These results demonstrate the potential of our work to model, for example, how an optimal persister strategy interacts with therapeutic interventions such as drug sequencing (44, 45).

Discussion

In this work, we model persister dynamics using a stochastic model and introduce the idea of *cellular hedging* to study an optimal persister production strategy. By applying cross-disciplinary ideas from mathematical finance to the persister problem, we provide several analytical and simulation results to elucidate bacterial persistence under different forms of environmental volatility.

Our model suggests that it is detrimental to produce persisters in the absence of volatility. In examining the optimal strategy for constant persister production, we reveal the proportion of persisters that can be maintained to maximise the expected growth of the population (Eq. 14). Removing volatility from the model by using constant expected growth rate and setting $\sigma = 0$, recovers the deterministic model of Balaban *et al.* (10) and reveals an optimal persister proportion of zero. Therefore, our model predicts that producing persisters in the absence of environmental volatility is sub-optimal and, therefore, leads to a lower expected per-capita growth rate. In contrast, our straightforward assumption of Wiener noise in the growth rate reveals a small proportion of persisters (approximately 1 in 10^5) — consistent with experimental observations of Balaban *et al.* (10) — that maximises the expected per-capita growth rate. This result contrasts with previous mathematical studies that assume external factors, such as antibiotic treatment, to explain persistence (21).

Compared to financial hedging, cellular hedging differs significantly in the complexity of the strategy that can be implemented. A key result is our direct comparison of bacterial persistence and MPP revealing a constant optimal proportion of persisters that should be maintained in an environment with a constant expected growth rate. This result is significant for the persister problem as, unlike in MPP, the cell population cannot directly control the proportion of persisters. However, the population can maintain a constant *expected* population, regulated by constant switching propensities, u and v.

The mechanisms that enable cells to implement cellular hedging strategies that respond to the environment are unknown (46), but they must come at a cost to the cells in terms of additional genetic machinery and rely on limited information available to individual bacteria. Our study reveals an optimal variable persister production strategy that depends only on the time, persister proportion and the environment, but not on the the population size. Additional results in the supporting material (Fig. S6) also indicate that these strategies become time-independent far from the terminal time, T. Furthermore, the strategy itself is not complex. Rather, bacteria increase persisters production when the persister proportion for a given growth rate is less than optimal. These results are surprising as optimal control theory only provides the strategy that maximises the payoff, and does not necessarily enforce any level of complexity in the cellular hedging strategy.

Our model suggests new experimental pathways to understand persistence. Rapid evolution of cellular hedging strategies is experimentally reproducible (47): Van den Bergh *et al.* (14) found that exposing *E. coli* to daily antibiotic treatments increased survival by between three and 300-fold after just three treatments, and Rodriguez-Beltran *et al.* (48) study induced evolutionary changes in bacteria behaviour through repeated application of antibiotics. An experimental study where bacteria are repeatedly exposed to a known volatile environment, potentially based upon the Monod or Poisson environment which we study, will provide insight into how bacteria adapt to uncertainty. Our modelling framework can then predict both the emergent strategy and how the population might behave when exposed to interventions such as antibiotics. Furthermore, financial mathematics techniques may be applied to study the evolutionary process as it occurs. For example, policy adjustment models (49) quantify the cost of strategy change, and can be compared to mutation costs in a rapidly-evolving cell colony.

In Fig. 3 we simulate a persister producing bacteria colony under antibiotic treatment, demonstrating the distinct advantage persisters afford bacteria (10, 14, 17). Our stochastic model of persister production can be used to improve the efficacy of antimicrobial therapies using optimal control from an optimal treatment perspective (43, 50, 51). Furthermore, recent experimental and mathematical work examines the potential of so-called *evolutionarily informed therapy* or *drug sequencing* (44, 45, 52), where a sequence of drugs are administered to sequentially induce susceptibility and overcome drug resistance. As demonstrated in Fig. 3 and Fig. S2, our model allows simulation of how a population specialised to one environment could behave under another. Therefore, our framework may naturally extend to predict how a persister strategy optimal under one type of drug behaves under another. Our results already suggest new ways to design treatment strategies. Supplementary results (Fig. S6) suggest that, for all environments we model, persister production decreases monotonically with the growth rate. Temporarily

exposing the cell colony to favorable conditions may, therefore, decrease the variable persister production, lowering the proportion of persisters, thereby making the population more susceptible to antibiotics. This is consistent with existing experimental observations where exposing a colony to a fresh growth medium before applying antibiotics decreases persistence (53), and is a simplistic example of drug sequencing.

Conclusion

We provide new insight into cellular hedging by introducing a bridge between the study of biological population dynamics and the mathematics of financial risk management. A fundamental result of our study is to provide a solid theoretical understanding of why persistence is only advantageous in the presence of environmental volatility. Our analysis demonstrates that the study of this phenomenon must take a stochastic perspective. We present a new stochastic model of bacteria growth in a volatile environment and apply optimal control theory to probe the persister strategy that maximises the per-capita growth rate. Our model of cellular hedging has clinical significance and can be applied to improve the efficacy of antimicrobial therapies. Furthermore, the framework we develop can be applied to more complex models of bacterial population dynamics, and offers an opportunity for future generalisations to explore cellular decision making in a broader context. Many seemingly complex cellular phenomena from bet-hedging in cancers (7, 54, 55), herpes viruses (56) and HIV (57) to decision making in the epithelial-mesenchymal transition (58) can be modelled using ideas from cellular hedging and by furthering the unification of mathematical finance and biology.

References

[1] Bigger, J. W., 1944. Treatment of staphylococcal infections with penicillin by intermittent sterilisation. *The Lancet* 244:497–500.

[2] Veening, J.-W., W. K. Smits, and O. P. Kuipers, 2008. Bistability, epigenetics, and bet-hedging in bacteria. *Annu. Rev. Microbiol.* 62:193–210.

[3] Merton, R. C., 1971. Optimum Consumption and Portfolio Rules in a Continuous-Time Model. *J. Econ. Theory* 3:373–413.

[4] Wolf, D. M., V. V. Vazirani, and A. P. Arkin, 2005. Diversity in times of adversity: probabilistic strategies in microbial survival games. *J. Theor. Biol.* 234:227–253.

[5] Williams, P. D., and A. Hastings, 2011. Paradoxical persistence through mixed-system dynamics: towards a unified perspective of reversal behaviours in evolutionary ecology. *Proc. R. Soc. B* 278:1281–1290.

[6] Jia, C., M. Qian, Y. Kang, and D. Jiang, 2014. Modeling stochastic phenotype switching and bet-hedging in bacteria: stochastic nonlinear dynamics and critical state identification. *Quant. Biol.* 2:110–125.

[7] Nichol, D., M. Robertson-Tessi, P. Jeavons, and A. R. A. Anderson, 2016. Stochasticity in the Genotype-Phenotype Map: Implications for the Robustness and Persistence of Bet-Hedging. *Genetics* 204:1523–1539.

[8] Ardaševa, A., R. A. Gatenby, A. R. A. Anderson, H. M. Byrne, P. K. Maini, and T. Lorenzi, 2020. Evolutionary dynamics of competing phenotype-structured populations in periodically fluctuating environments. *J. Math. Biol.* 80:775–807.

[9] Martín, P. V., M. A. Muñoz, and S. Pigolotti, 2019. Bet-hedging strategies in expanding populations. *PLoS Comput. Biol.* 15:e1006529.

[10] Balaban, N. Q., J. Merrin, R. Chait, L. Kowalik, and S. Leibler, 2004. Bacterial persistence as a phenotypic switch. *Science* 305:1622–1625.

[11] Brauner, A., N. Shoresh, O. Fridman, and N. Q. Balaban, 2017. An Experimental Framework for Quantifying Bacterial Tolerance. *Biophys. J.* 112:2664–2671.

[12] Şimşek, E., and M. Kim, 2019. Power-law tail in lag time distribution underlies bacterial persistence. *Proc. Natl. Acad. Sci. U.S.A.* 116:17635–17640.

[13] Barrett, T. C., W. W. K. Mok, A. M. Murawski, and M. P. Brynildsen, 2019. Enhanced antibiotic resistance development from fluoroquinolone persisters after a single exposure to antibiotic. *Nat. Commun.* 1–11.

[14] Van den Bergh, B., J. E. Michiels, T. Wenseleers, E. M. Windels, P. V. Boer, D. Kestemont, L. D. Meester, K. J. Verstrepen, N. Verstraeten, M. Fauvart, and J. Michiels, 2016. Frequency of antibiotic application drives rapid evolutionary adaptation of *Escherichia coli* persistence. *Nat. Microbiol.* 1:16020.

[15] Bartell, J. A., L. M. Sommer, J. A. J. Haagensen, A. Loch, R. Espinosa, S. Molin, and H. K. Johansen, 2019. Evolutionary highways to persistent bacterial infection. *Nat. Commun.* 10:629.

[16] Fauvart, M., V. N. D. Groote, and J. Michiels, 2011. Role of persister cells in chronic infections: clinical relevance and perspectives on anti-persister therapies. *J. Med. Microbiol.* 60:699–709.

[17] Windels, E. M., J. E. Michiels, M. Fauvart, T. Wenseleers, B. van den Bergh, and J. Michiels, 2019. Bacterial persistence promotes the evolution of antibiotic resistance by increasing survival and mutation rates. *ISME J.* 13:1239–1251.

[18] Amato, S. M., M. A. Orman, and M. P. Brynildsen, 2013. Metabolic Control of Persister Formation in Escherichia coli. *Mol. Cell* 50:475–487.

[19] Harms, A., E. Maisonneuve, and K. Gerdes, 2016. Mechanisms of bacterial persistence during stress and antibiotic exposure. *Science* 354:aaf4268.

[20] Moyed, H. S., and K. P. Bertrand, 1983. *hipA*, a newly recognized gene of *Escherichia coli* K-12 that affects frequency of persistence after inhibition of murein synthesis. *J. Bacteriol.* 155:768–775.

[21] Kussell, E., R. Koshony, N. Q. Balaban, and S. Leibler, 2005. Bacterial Persistence: A Model of Survival in Changing Environments. *Genetics* 169:1807–1814.

[22] Alonso, A. A., I. Molina, and C. Theodoropoulos, 2014. Modeling bacterial population growth from stochastic single-cell dynamics. *Appl. Environ. Microbiol.* 80:5241–5253.

[23] Øksendal, B., 1998. Stochastic Differential Equations. Springer, Berlin, Heidelberg.

[24] Merton, R. C., 1973. Theory of rational option pricing. *Bell J. Econ.* 4:141.

[25] Black, F., and M. Scholes, 1973. The pricing of options and corporate liabilities. *J. Political Econ.* 81:637–654.

[26] Gaál, B., J. W. Pitchford, and A. J. Wood, 2010. Exact Results for the Evolution of Stochastic Switching in Variable Asymmetric Environments. *Genetics* 184:1113–1119.

[27] Müller, J., B. A. Hense, T. M. Fuchs, M. Utz, and C. Pötzsche, 2013. Bet-hedging in stochastically switching environments. *J. Theor. Biol.* 336:144–57.

[28] Hanson, F. B., 2007. Applied stochastic processes and control for jump diffusions. SIAM.

[29] Garcia-Bernardo, J., and M. Dunlop, 2015. Noise and Low-Level Dynamics Can Coordinate Multicomponent Bet Hedging Mechanisms. *Biophys. J.* 108:184–193.

[30] Varughese, M. M., and L. P. Fatti, 2008. Incorporating environmental stochasticity within a biological population model. *Theor. Popul. Biol.* 74:115–129.

[31] Thattai, M., and A. van Oudenaarden, 2004. Stochastic gene expression in fluctuating environments. *Genetics* 167:523–530.

[32] Acar, M., J. T. Mettetal, and A. van Oudenaarden, 2008. Stochastic switching as a survival strategy in fluctuating environments. *Nat. Genet.* 40:471–475.

[33] Maisonneuve, E., and K. Gerdes, 2014. Molecular Mechanisms Underlying Bacterial Persisters. *Cell* 157:539–548.

[34] Feng, J., D. A. Kessler, E. Ben-Jacob, and H. Levine, 2014. Growth feedback as a basis for persister bistability. *Proc. Natl. Acad. Sci. U.S.A.* 111:544–549.

[35] Pai, A., and L. You, 2009. Optimal tuning of bacterial sensing potential. *Mol. Syst. Biol.* 5:1–11.

[36] Ghosh, A., Ö. Baltekin, M. Wäneskog, D. Elkhalifa, D. L. Hammarlöf, J. Elf, and S. Koskiniemi, 2018. Contact-dependent growth inhibition induces high levels of antibiotic-tolerant persister cells in clonal bacterial populations. *EMBO J.* 37:e98026.

[37] Roberts, M. E., and P. S. Stewart, 2005. Modelling protection from antimicrobial agents in biofilms through the formation of persister cells. *Microbiology* 151:75–80.

[38] Cogan, N. G., 2006. Effects of persister formation on bacterial response to dosing. *J. Theor. Biol.* 238:694–703.

[39] Carvalho, G., D. Balestrino, C. Forestier, and J.-D. Mathias, 2018. How do environment-dependent switching rates between susceptible and persister cells affect the dynamics of biofilms faced with antibiotics? *NPJ Biofilms Microbi.* 4:1–8.

[40] Jablonka, E., B. Oborny, I. Molnár, E. Kisdi, J. Hofbauer, and T. Czárán, 1995. The adaptive advantage of phenotypic memory in changing environments. *Philos. T. R. Soc. B* 350:133–141.

[41] Tourigny, D. S., 2020. Dynamic metabolic resource allocation based on the maximum entropy principle. *J. Math. Biol.* 80:2395–2430.

[42] Higham, D. J., 2001. An Algorithmic Introduction to Numerical Simulation of Stochastic Differential Equations. *SIAM Rev.* 43:525–546.

[43] Sharp, J. A., A. P. Browning, T. Mapder, K. Burrage, and M. J. Simpson, 2019. Optimal control of acute myeloid leukaemia. *J. Theor. Biol.* 470:30–42.

[44] Maltas, J., and K. B. Wood, 2019. Pervasive and diverse collateral sensitivity profiles inform optimal strategies to limit antibiotic resistance. *PLoS Biol.* 17:e3000515.

[45] Nichol, D., J. Rutter, C. Bryant, A. M. Hujer, S. Lek, M. D. Adams, P. Jeavons, A. R. A. Anderson, R. A. Bonomo, and J. G. Scott, 2019. Antibiotic collateral sensitivity is contingent on the repeatability of evolution. *Nat. Commun.* 10:334.

[46] Rotem, E., A. Loinger, I. Ronin, I. Levin-Reisman, C. Gabay, N. Shoresh, O. Biham, and N. Q. Balaban, 2010. Regulation of phenotypic variability by a threshold-based mechanism underlies bacterial persistence. *Proc. Natl. Acad. Sci. U.S.A.* 107:12541–12546.

[47] Beaumont, H. J. E., J. Gallie, C. Kost, G. C. Ferguson, and P. B. Rainey, 2009. Experimental evolution of bet hedging. *Nature* 461:90–93.

[48] Rodriguez-Beltran, J., J. C. R. Hernandez-Beltran, J. DelaFuente, J. A. Escudero, A. Fuentes-Hernandez, R. C. MacLean, R. Peña-Miller, and A. S. Millan, 2018. Multicopy plasmids allow bacteria to escape from fitness trade-offs during evolutionary innovation. *Nat. Ecol. Evol.* 2:873—881.

[49] Boettiger, C., M. Bode, J. N. Sanchirico, J. Lariviere, A. Hastings, and P. R. Armsworth, 2016. Optimal management of a stochastically varying population when policy adjustment is costly. *Ecol. Appl.* 26:808–817.

[50] Cogan, N. G., J. Brown, K. Darres, and K. Petty, 2012. Optimal control strategies for disinfection of bacterial populations with persister and susceptible dynamics. *Antimicrob. Agents. Ch.* 56:4816–4826.

[51] Sharp, J. A., A. P. Browning, T. Mapder, K. Burrage, and M. J. Simpson, 2020. Designing combination therapies using multiple optimal controls. *J. Theor. Biol.* 497:110277.

[52] Nichol, D., P. Jeavons, A. G. Fletcher, R. A. Bonomo, P. K. Maini, J. L. Paul, R. A. Gatenby, A. R. Anderson, and J. G. Scott, 2015. Steering Evolution with Sequential Therapy to Prevent the Emergence of Bacterial Antibiotic Resistance. *PLoS Comput. Biol.* 11:e1004493.

[53] Gefen, O., C. Gabay, M. Mumcuoglu, G. Engel, and N. Q. Balaban, 2008. Single-cell protein induction dynamics reveals a period of vulnerability to antibiotics in persister bacteria. *Proc. Natl. Acad. Sci. U.S.A.* 105:6145–6149.

[54] Haass, N. K., K. A. Beaumont, D. S. Hill, A. Anfosso, P. Mrass, M. A. Munoz, I. Kinjyo, and W. Weninger, 2014. Real-time cell cycle imaging during melanoma growth, invasion, and drug response. *Pigment Cell. Melanoma Res.* 27:764–776.

[55] Kaznatcheev, A., J. Peacock, D. Basanta, A. Marusyk, and J. G. Scott, 2019. Fibroblasts and alectinib switch the evolutionary games played by non-small cell lung cancer. *Nat. Ecol. Evol.* 3:450–456.

[56] Stumpf, M. P. H., Z. Laidlaw, and V. A. A. Jansen, 2002. Herpes viruses hedge their bets. *Proc. Natl. Acad. Sci. U.S.A.* 99:15234–15237.

[57] Rouzine, I. M., A. D. Weinberger, and L. S. Weinberger, 2015. An evolutionary role for HIV latency in enhancing viral transmission. *Cell* 160:1002–12.

[58] Lu, M., M. K. Jolly, H. Levine, J. N. Onuchic, and E. Ben-Jacob, 2013. MicroRNA-based regulation of epithelial-hybrid-mesenchymal fate determination. *Proc. Natl. Acad. Sci. U.S.A.* 110:18144–18149.

Acknowledgements

This work is supported by the Australian Research Council (DP170100474) and the Air Force Office of Scientific Research (BAA-AFRL-AFOSR-2016-0007).

Author Contributions

All authors designed the research; A.P.B. performed the research and wrote the manuscript; A.P.B., T.M., and J.A.S. implemented the numerical techniques. All authors provided direction, feedback and gave approval for final publication.

Competing Interests

The authors declare no competing interests.

Data availability

This study contains no experimental data. Code used to produce the numerical results is available on GitHub at `github.com/ap-browning/persisters`.